

Whole-body biodistribution, radiation dosimetry estimates for the PET norepinephrine transporter probe (S,S)-[¹⁸F]FMeNER-D₂ in non-human primates

Nicholas Seneca^{a,b}, Bengt Andree^a, Nils Sjöholm^a, Magnus Schou^a, Stefan Pauli^a, P. David Mozley^c, James B. Stubbs^d, Jieh-San Liow^b, Judit Sovago^a, Balazs Gulyás^a, Robert Innis^b and Christer Halldin^a

Background (S,S)-[¹⁸F]FMeNER-D₂ is a recently developed norepinephrine transporter ligand which is a potentially useful radiotracer for mapping the brain and heart norepinephrine transporter *in vivo* using positron emission tomography. In this work, we quantified the biodistribution over time and radiation exposure to multiple organs with (S,S)-[¹⁸F]FMeNER-D₂.

Methods Whole-body images were acquired for 21 time points in two cynomolgus monkeys for approximately 270 min after injection of radioligand. Compressed 3-D to 2-D planar images were used to identify organs with the highest radiation exposure at each time point. Estimates of the absorbed dose of radiation were calculated using the MIRDose 3.1 software program performed with the dynamic bladder and ICRP 30 gastrointestinal tract models.

Results In planar images, peak values of the percent injected dose (%ID) at a time after radioligand injection were calculated for the lungs (26.76% ID at 1.42 min), kidneys (13.55% ID at 2.18 min), whole brain (5.65% ID at 4.48 min), liver (7.20% ID at 2 min), red bone marrow (5.02% ID at 2.06 min), heart (2.36% ID at 1.42 min) and urinary bladder (23% ID at 250 min). Assuming a urine voiding interval of 2.4 h, the four organs with highest exposures in $\mu\text{Gy} \cdot \text{MBq}^{-1}$ ($\text{mrad} \cdot \text{mCi}^{-1}$) were kidneys 126 (468),

heart wall 108 (399), lungs 88.4 (327) and urinary bladder 114 (422). The effective doses were estimated with and without urine voiding at a range of 123 (33) and to 131 (35.5) $\mu\text{Gy} \cdot \text{MBq}^{-1}$ ($\text{mrad} \cdot \text{mCi}^{-1}$).

Conclusion The estimated radiation burden of (S,S)-[¹⁸F]FMeNER-D₂ is comparable to that of other ¹⁸F radioligands. *Nucl Med Commun* 26:695–700 © 2005 Lippincott Williams & Wilkins.

Nuclear Medicine Communications 2005, 26:695–700

Keywords: (S, S)-[¹⁸F]FMeNER-D₂, norepinephrine transporter, dosimetry, whole-body biodistribution, PET, positron emission tomography

^aKarolinska Institutet, Department of Clinical Neuroscience, Karolinska Hospital, Stockholm, Sweden, ^bMolecular Imaging Branch, National Institute of Mental Health, National Institutes of Health, Bethesda, Maryland, USA, ^cEli Lilly Co., Indianapolis, USA and ^dRadiation Dosimetry Systems, Inc. Alpharetta, Georgia, USA.

Nicholas Seneca and Magnus Schou were supported by a grant from the NIH-KI joint PhD programme.

Correspondence to Dr Nicholas Seneca, Karolinska Institutet, Department of Clinical Neuroscience, Psychiatry Section, Karolinska Institute and Hospital, S-171 76 Stockholm, Sweden.
Tel: +46 517 72997; fax: +46 8 517 71753;
e-mail: Nick.Seneca@cns.ki.se

Received 18 November 2004 Accepted 30 March 2005

Introduction

The norepinephrine transporter (NET) is a carrier protein that transports norepinephrine across the pre-synaptic membrane. NET terminates the action of norepinephrine in the synapse via re-uptake and thus regulates norepinephrine neurotransmission. Abnormalities in brain norepinephrine are associated with a variety of neuropsychiatric conditions characterized by cognitive dysfunction and mood disorders [1–3]. NET radioligands may also measure the in-vivo function of cardiac synaptic neurotransmission, considering the noradrenergic neuron distribution in the peripheral autonomic nervous system [4,5]. These factors have made the norepinephrine system an important research topic in neuroscience, neuroimaging, cardiac imaging and drug development [6–9].

The measurement of regional NET levels in brain has been hampered by the lack of suitable PET radioligands for NET. Evaluation of the ¹¹C labelled ($T_{1/2} = 20.4$ min) *O*-methyl reboxetine analogue, (S,S)-[¹¹C]MeNER, showed that specific binding to NET did not reach maximal values (i.e., equilibrium) during the PET scanning session of 93 min [10–12]. This, together with a somewhat noisy final signal at later time points, are relative deficiencies of (S,S)-[¹¹C]MeNER for the quantitative studies of NET in brain.

Recently, the preparation and evaluation of two novel radiofluorinated analogues of (S,S)-[¹¹C]MeNER have been reported [13]. PET examination revealed skull-bound radioactivity, contaminating images of the brain and indicating fast defluorination of the radioligand [13].

This defluorination was reduced by the addition of a di-deuterated analogue in PET experiments with (*S,S*)-[¹⁸F]FMeNER-D₂. The use of the latter compound has demonstrated that the in-vivo defluorination rate of aryl fluoromethoxy compounds can be reduced through the deuterium isotope effect [14,15]. The di-deutero radioligand (*S,S*)-[¹⁸F]FMeNER-D₂, was therefore used in the present study, which allows for a lower dose to the bone marrow and is superior to (*S,S*)-[¹¹C] MeNER given that a specific binding peak equilibrium is reached during the PET experiment at a lower noise level.

In addition to the importance of imaging NET in brain, visualization of NET may aid in understanding the pathophysiology of several neurocardiac disorders. Cardiac imaging has several clinical implications including therapeutic management of patients suffering from cardiovascular diseases, progression of orthostatic hypotension in Parkinson's disease patients, and providing insight into heart function [16]. Further insight into heart failure with PET would provide a diagnostic tool to identify chronic heart failure early in the disease process, examine underlying conditions to worsening symptoms and an additional diagnostic tool to possibly identify people who are at high risk of developing a heart condition.

Several radioligands for norepinephrine have been studied in the heart with positron emission tomography (PET) and single photon emission computed tomography (SPECT). Initial PET studies with ¹¹C-norepinephrine showed rapid high uptake of radioactivity in the heart of a monkey [17]. Following pretreatment with desipramine, a selective inhibitor of norepinephrine re-uptake, the uptake of radioactivity in the myocardium was markedly reduced [15]. PET experiments with 4-[¹⁸F]FMR and 6-[¹⁸F]FMR have demonstrated similar affinity towards myocardial norepinephrine transport mechanisms as well as significant reduction in binding following pretreatment with desipramine [18].

The first clinical application by SPECT was with ¹²³I-MIBG, which showed high uptake in the heart due to the dense sympathetic innervation [16]. The essential irreversible uptake into the cytoplasm and the noradrenergic storage in vesicles has made this technique difficult to quantify. The development and use of more efficient NET radioligands in studies of the heart with PET and SPECT may, however, lead to a better understanding of the cardiac sympathetic nervous function.

An important safety as well as limiting factor for the clinical usability of a radioligand is set by the relationship between radiation absorbed doses in different source organs of the body following the radioactivity dose injected. The amount of the radiation absorbed dose

delivered by internal administration radiopharmaceuticals is based on the fact that radiopharmaceuticals have a certain biological, physical and effective half-life based on the radionuclide half-lives. ¹⁸F decays predominantly, but not exclusively, by positron (β^+) emission and has a half-life of 109.7 min. Dosimetry evaluations for radionuclides with longer half-lives should take into account the times at which radioactivity accumulation is observed in source organs and the biological half-times for accumulation and clearance.

The aims of the present study were to measure the whole-body biodistribution over time of (*S,S*)-[¹⁸F]FMeNER-D₂ and to estimate the resulting radiation exposure to organs of the body. Absorbed doses were estimated following the administration of (*S,S*)-[¹⁸F]FMeNER-D₂ and calculated from cynomolgus monkey biodistribution data. The MIRD scheme was applied as an accurate determination of the time-dependent activity of the target regions of the body.

Methods and materials

Radiochemistry

(*S,S*)-[¹⁸F]FMeNER-D₂ was prepared as described in detail elsewhere [13]. The precursor and standard of FMeNER-D₂ were supplied by Eli Lilly, Indianapolis, USA. Other chemicals were obtained from commercial sources and were of analytical grade. Radiochemical purity was higher than 99% in each of the two batches. The specific radioactivity was higher than $148 \times 10^3 \text{ GBq} \cdot \text{mmol}^{-1}$ ($4000 \text{ Ci} \cdot \text{mmol}^{-1}$) and the mass injected was less than 0.1 μg .

Animals

Two female cynomolgus monkeys (2.65 and 2.85 kg) were supplied by the National Institute for Infectious Disease Control, SMI, Solna, Sweden. The study was approved by the Animal Research Ethical Committee of the Northern Stockholm Region. Principles of laboratory animal care was followed according to NIH publication No. 85-23, revised 1985.

Anaesthesia was induced and maintained every 40 min by repeated intramuscular injections of a mixture of ketamine ($3\text{--}4 \text{ mg} \cdot \text{kg}^{-1} \cdot \text{h}^{-1}$; Ketalar, Parke-Davis) and xylazine hydrochloride ($1\text{--}2 \text{ mg} \cdot \text{kg}^{-1} \cdot \text{h}^{-1}$; Rompun Vet., Bayer, Sweden) for the duration of each scanning experiment. Body temperature was controlled by Bair Hugger, Model 505 (Arizant Healthcare Inc., Minnesota, USA). A urinary catheter was inserted and clamped so that the radioactivity overlaying the bladder represented the total urinary excretion during the scanning interval. Electrocardiogram (ECG) measurements were performed before and 10 min after radioligand injection. Heart and respiration rates were measured throughout the experiment.

Data acquisition

Whole-body transmission and emission scans were acquired on a Siemens ECAT EXACT HR PET system, which was run in the two-dimensional mode. The spatial resolution is about 6.0 mm full width at half maximum and the field of view 10.8 cm. Two whole-body transmission scans followed by emission scans, one for each monkey, were performed following the intravenous administration of (*S,S*)-[¹⁸F]FMeNER-D₂, 65 and 76.4 MBq.

Serial dynamic transaxial images were acquired for a total of approx. 4.5 h (including dead time) from six bed positions from head to mid-tail. The acquisition during PET measurement started immediately following radioligand injection. The overlap between sections during PET measurements corresponds to five planes (~1.5 cm). The acquisition sequence for each frame consisted of the following: starting an emission scan at the first bed position for the head, moving the bed caudally to the next section, scanning a total of six sections consecutively for the same period of time with six 7-s intervals to move the bed and 21 s to reposition the bed back to the first section after completing the frame. Each of the six sections corresponding to a total field of view between 46 and 55 cm of the body, was imaged 21 times with the following sequence of frame acquisitions: 4 × 0.50 min, 6 × 1 min, 5 × 2 min and 6 × 4 min. Each frame includes 31 planes (3.125 mm thickness).

Transmission scan for attenuation correction

For transmission correction of the data, a 3 min scan for each bed position, obtained with three rotating ⁶⁸Ge/⁶⁸Ga line sources were used. The raw PET data were then reconstructed using the standard filtered back-projection. The following reconstruction parameters were used: 3 mm Hanning filter, scatter correction, a zoom factor of 2 and a 128 × 128 array size.

Image and data analysis

The compressed planar images were created as previously described [19]. The planar images were analysed with PMOD 2.5 (pixel-wise modelling computer software; PMOD Group, Zurich, Switzerland). Urinary bladder, brain, kidneys, liver, vertebra, heart and lungs were identified on the emission images. Regions of interest (ROIs) were drawn on the planar images and a single generous-sized ROI was drawn over the total body and each organ.

Activity in the source organs (not decay corrected) were expressed as a percentage of injected dose and plotted versus time. The recovery of radioactivity was calculated from planar images as the percentage of injected activity in two monkeys. Radiation absorbed doses were calculated by multiplying each organ activity by 100 divided by

the percentage of recovered radioactivity in each of the two experiments. Thus, recovered activity was used to calculate per cent injected dose and residence times of different organs. The residence times from the monkey were calculated by converting the corresponding human values by multiplication with a factor to scale organ and body weights (in kg) as $(w_{m,b}/w_{m,o})(w_{h,o}/w_{h,b})$, where $w_{m,b}$ is the monkey body weight, $w_{m,o}$ is the monkey organ weight, $w_{h,b}$ is the human body weight, and $w_{h,o}$ is the human organ weight. This allometric scaling factor is identical to that using the standard uptake value (SUV), which expresses uptake as (%ID per g organ) × (body weight, in grams). That is, the scaling used in this paper assumes the SUV in the monkey organ is equal to that in the human organ.

Absorbed dose calculations

Time–activity curves were generated for each monkey for the seven identified source organs, including remainder of activity. Target organ absorbed radiation doses, effective dose and effective dose equivalent were calculated by MIRDOSE 3.1 [20]. Input data for MIRD scheme were calculated for each monkey and average values were used to calculate the extrapolated human data. The mean cumulative urine activities from two animals were fitted with a mono-exponential curve to estimate the percentage of injected dose excreted via this route. The dynamic bladder model, implemented in MIRDOSE 3.1 software, was applied to calculate residence time of the urinary activity with voiding intervals of 2.4 h, 4.8 h and no urine voiding [21].

Results

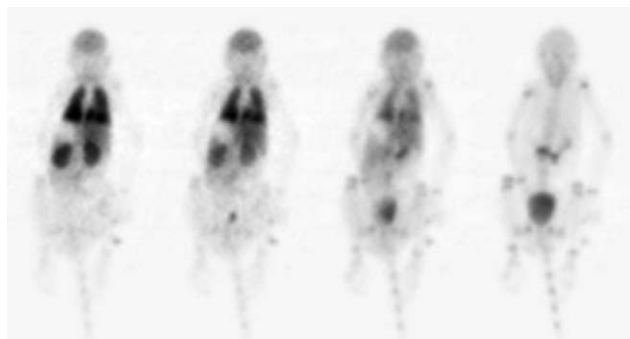
Injection of (*S,S*)-[¹⁸F]FMeNER-D₂ caused no change in ECG, heart or respiration rates. Recovery of radioactivity from planar images was 90% and 91% of the injected activity in the two monkeys. Recovered activity was used to calculate per cent injected dose and residence times of different organs.

Biodistribution

On the whole-body emission images, urinary bladder, brain, kidneys, liver, lungs, entire abdomen (GI tract) and vertebra were visually identified as organs with moderate to high activity (Fig. 1). In planar images, the peak values of the per cent injected dose to the lungs, kidneys, brain, liver, red bone marrow, heart and urinary bladder were 26.8%, 13.6%, 5.7%, 7.2%, 5.0%, 2.4% and 23% at peak times 1.42, 2.18, 4.48, 2, 2.06, 1.42 and 250 min, respectively (Fig. 2(A and B)).

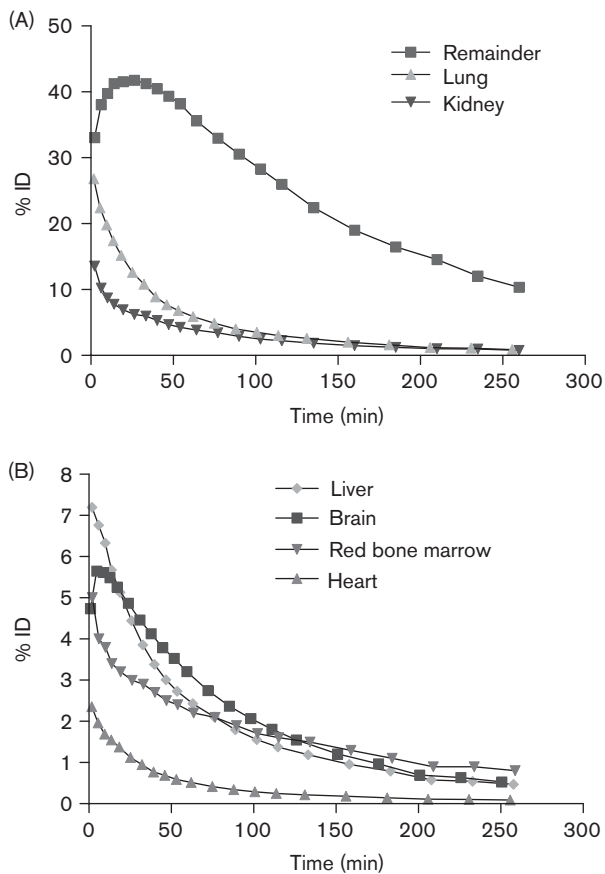
Time–activity curve for (*S,S*)-[¹⁸F]FMeNER-D₂ as determined by PET imaging of bladder after radioactive decay correction are shown for monkey 2 in Fig. 3. The cumulative urinary excretion of (*S,S*)-[¹⁸F]FMeNER-D₂ was 20.8% at 150 min. The data from 0 to 150 min was

Fig. 1



Whole-body images demonstrating biodistribution of (S,S)-[¹⁸F]FMeNER-D₂ in monkey 2 at 3, 8, 30 and 110 min after radioligand injection.

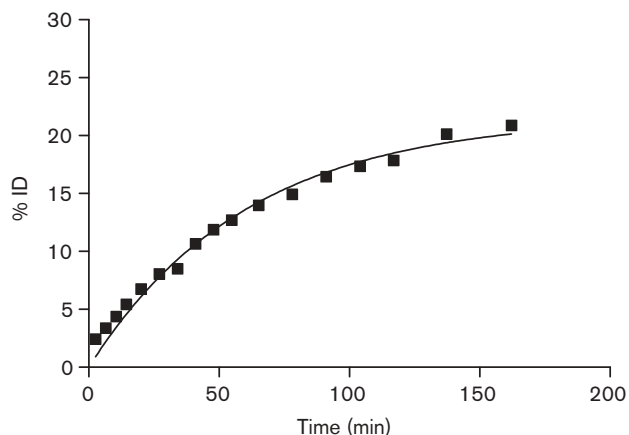
Fig. 2



Mean organ uptake over time without decay correction, expressed as a percentage of injected dose (%ID) of (S,S)-[¹⁸F]FMeNER-D₂ on planar images.

fitted to an exponential curve fitting due to urine excretion after 150 min, which would have led to an underestimation of urine activity. This activity was fitted

Fig. 3



Time-activity curve for (S,S)-[¹⁸F]FMeNER-D₂ as determined by PET imaging of bladder. Data are expressed for monkey 2 and are corrected for radioactive decay. The curve overlying the measured data points represents a mono-exponential fitting with an asymptote of 24% of urine activity in bladder at infinite time.

with a mono-exponential association curve (Fig. 3), and the urinary excretion rate was calculated with $R^2 = 0.98$ for the determined values of the two monkeys. The exponential fitting for the average of the two monkeys showed an asymptotic maximal value of about 24% urinary excretion at infinite time. The effective half-life was estimated to be 0.649 h on the basis of the dynamic bladder uptake.

The liver showed a relatively rapid elimination shown in Fig. 2(B). About two thirds of the injected activity went from the liver to the gastrointestinal tract during the first 4 h after administration of (S,S)-[¹⁸F]FMeNER-D₂. The elimination would lead to relatively low radiation exposure to organs in the lower part of the body due to the short half-life of ¹⁸F and the transit through the gastrointestinal tract.

Radiation absorbed dose estimates

Human residence times were extrapolated from planar images using the average of two monkeys (Table 1). Radiation absorbed dose estimates were calculated with MIRDOSE 3.1 computer program, with urine voiding intervals of 2.4 h, 4.8 h and no voiding (Table 2). Assuming a urine voiding interval of 2.4 h the activity in the urinary bladder was 114 $\mu\text{Gy} \cdot \text{MBq}^{-1}$ (422 $\text{mrad} \cdot \text{mCi}^{-1}$), at 4.8 h the activity was 167 $\mu\text{Gy} \cdot \text{MBq}^{-1}$ (619 $\text{mrad} \cdot \text{mCi}^{-1}$) and at no urine voiding the activity increased to 186 $\mu\text{Gy} \cdot \text{MBq}^{-1}$ (688 $\text{mrad} \cdot \text{mCi}^{-1}$) (Table 2). Minimal change was seen in other organs at the various urine voiding intervals. The effective dose

was estimated to be $33.2 \mu\text{Sv} \cdot \text{MBq}^{-1}$ and $34.3 \mu\text{Sv} \cdot \text{MBq}^{-1}$, with 2.4 h and 4.8 h voiding intervals (Table 2).

Discussion

This study estimated the radiation absorbed dose resulting from the i.v. injection of (*S,S*)- ^{18}F FMENER-D₂. The four organs with highest exposures were kidneys, heart wall, lungs and urinary bladder. The absorbed radiation dose to the urinary bladder wall was calculated using voiding intervals of 2.4 h, 4.8 h and no voiding [19,20]. The use of planar images for the data analysis provided conservative estimates of radiation exposure, since the large regions of interest included overlying tissues.

The calculated dosimetry results seem comparable with those for other ^{18}F labelled brain imaging agents [22,23].

Table 1 Human residence times for (*S,S*)- ^{18}F FMENER-D₂ extrapolated from the average of two cynomolgus monkeys calculated from whole-body planar images

Organ	Residence time (h)
Brain	0.15
Heart	0.17
Lung	0.47
Kidney	0.19
Liver	0.16
Red bone marrow	0.17
Remainder of body	1.08

Table 2 Radiation dosimetry estimates for (*S,S*)- ^{18}F FMENER-D₂ extrapolated from the mean of the two monkey data estimated for human

Target organ	Voiding 2.4 h		Voiding 4.8 h		Without voiding	
	$\mu\text{Gy} \cdot \text{MBq}^{-1}$	mrad $\cdot \text{mCi}^{-1}$	$\mu\text{Gy} \cdot \text{MBq}^{-1}$	mrad $\cdot \text{mCi}^{-1}$	$\mu\text{Gy} \cdot \text{MBq}^{-1}$	mrad $\cdot \text{mCi}^{-1}$
Adrenals	17.2	63.7	17.3	63.9	17.3	64
Brain	27.6	102	27.6	102	27.6	102
Breasts	9.82	36.3	9.83	36.4	9.83	36.4
Gallbladder wall	15.4	57.1	15.6	57.6	15.6	57.7
LLI Wall	15.8	58.3	17.3	64	17.8	66
Small intestine	26.2	96.8	26.8	99	27	99.7
Stomach	11.9	44.1	12	44.4	12	44.5
ULI wall	28.1	104	28.6	106	28.7	106
Heart wall	108	399	108	399	108	399
Kidneys	126	468	126	468	127	468
Liver	28.3	105	28.3	105	28.3	105
Lungs	88.4	327	88.4	327	88.4	327
Muscle	9.64	35.7	10	37.1	10.2	37.6
Ovaries	13.9	51.5	15.3	56.7	15.8	58.6
Pancreas	15.4	57	15.5	57.2	15.5	57.3
Red marrow	22.2	82	22.4	82.9	22.5	83.2
Bone surfaces	16	59.4	16.2	59.9	16.2	60.1
Skin	6.55	24.2	6.68	24.7	6.73	24.9
Spleen	13.3	49.1	13.3	49.3	13.3	49.4
Testes	8.1	30	9.12	33.8	9.48	35.1
Thymus	13.3	49.1	13.3	49.1	13.3	49.1
Thyroid	8.28	30.7	8.29	30.7	8.29	30.7
Urinary bladder wall	114	422	167	619	186	688
Uterus	16.8	62.1	20.1	74.4	21.3	78.6
Total body	13	48.2	13.4	49.6	13.5	50
Effective dose equivalent	43.2	160	46.8	173	48.1	178
Effective dose	33.2	123	34.3	127	35.5	131

The administration of (*S,S*)- ^{18}F FMENER-D₂ led to an effective dose of $0.033 \text{ mSv} \cdot \text{MBq}^{-1}$ ($123 \text{ mrem} \cdot \text{mCi}^{-1}$). Guidelines on radiation exposure for human subjects involved in research studies varies widely internationally. Careful risk–benefit regulations for healthy subjects participating in diagnostic procedures who will not benefit directly are set to reduce overall risk, maximize health and safety. These proposed regulations and recommendations lead to conservative estimations of dose limits.

Radiation risk estimates were recently introduced for the National Institutes of Health (NIH, Bethesda, Maryland, USA), stating that effective dose estimates considered the most accurate measure of radiation risks [24]. Based on revised NIH Clinical Center guidelines, a maximum of 50 mSv (5 rem) of effective dose per year for a research subject, for this limit corresponds to 1504 MBq ($\sim 41 \text{ mCi}$) per subject per year for (*S,S*)- ^{18}F FMENER-D₂.

The European Commission has established the medical exposures directive (97/43/Euratom) which contains three categories of effective dose ranges established for adults under 50 years of age [25]. Under these guidelines minor to intermediate risk levels correspond to effective dose ranges in adults of 1–10 mSv (0.1–1 rem) per annum. Based on these guidelines, the maximal limit of 10 mSv (1 rem) would result from an injected activity of 333 MBq ($\sim 9 \text{ mCi}$) (*S,S*)- ^{18}F FMENER-D₂ per subject per year.

The variability in international standards for maximal radiation exposure, thus may have implications for the clinical use of (*S,S*)-[¹⁸F]FMeNER-D₂ for multiple PET measurements. Considering these varying radiation safety standards, different limits for protection against radiation have been set for the USA and European Union (EU). While US standards have set the maximum radiation exposure at 5 rem per year, the EU has set a five times lower maximum radiation exposure for adults under the age of 50 years. For people over the age of 50, however, the EU allows an increase of radiation exposure by a factor of 5 to 10.

Alterations of NET density have been reported in several forms of cardiac failure [5,6], and PET NET radioligands may be useful to cardiac pathophysiology. In this study, tracer uptake into monkey heart was rapid, with maximum uptake of 2.5% of injected dose at approximately 2 min, although we are uncertain how much of this activity was in cardiac muscle compared to the vascular cavity. Uptake in heart was visually apparent in planar images up to 25 min after radioligand injection, with the majority of uptake in cardiac muscle itself. The activity at this later time point demonstrates that the uptake is predominately in the cardiac muscle. A future study with blocking doses of desipramine, a relatively selective NET inhibitor, will help determine the selectivity of (*S,S*)-[¹⁸F]FMeNER-D₂ binding in the heart.

Our findings indicate that (*S,S*)-[¹⁸F]FMeNER-D₂ may be a suitable radioligand for studying NET in the brain and as well as cardiac sympathetic innervation. The radiation exposure for each organ was found to be similar to other ¹⁸F labelled radioligands. These results in primates can be used to estimate the limit of radioactivity that can be administered at a low risk to human subjects. However, a human biodistribution study would provide more accurate estimation of organ radiation absorbed doses.

Acknowledgements

The authors would like to thank Lilly Research Laboratories for providing the precursors and standards. We are also grateful to the members of the Karolinska PET psychiatry group and nuclear medicine PET group. We gratefully acknowledge Dr Cyrill Burger for providing PMOD (version 2.5) software and Dr Dnyanesh Tipre, PhD for his valuable comments. James B. Stubbs performed the dosimetry analysis as a consultant to Eli Lilly & Company.

References

- McCormick DA, Pape HC, Williamson A. Actions of norepinephrine in the cerebral cortex and thalamus: implications for function of the central noradrenergic system. *Prog Brain Res* 1991; **88**:293–305.
- Mazei MS, Pluto CP, Kirkbride B, Pehek EA. Effects of catecholamine uptake blockers in the caudate-putamen and subregions of the medial prefrontal cortex of the rat. *Brain Res* 2002; **936**:58–67.
- Stahl SM. Neurotransmission of cognition, part 2. Selective NRIs are smart drugs: exploiting regionally selective actions on both dopamine and norepinephrine to enhance cognition. *J Clin Psychiatry* 2003; **64**:110–111.
- Goldstein DS, Brush JE, Eisenhofer G, Stull R, Esler M. *In vivo* measurement of neuronal uptake of norepinephrine in the human heart. *Circulation* 1988; **78**:41–48.
- Langer O, Halldin C. PET and SPET tracers for mapping the cardiac nervous system. *Eur J Nucl Med Mol Imaging* 2002; **29**:416–434.
- Melon P, Schwaiger M. Imaging of metabolism and autonomic innervation of the heart by positron emission tomography. *Eur J Nucl Med* 1992; **19**:453–464.
- Brunello N, Mendlewicz J, Kasper S, Leonard B, Montgomery S, Nelson J, et al. The role of noradrenaline and selective noradrenaline reuptake inhibition in depression. *Eur Neuropsychopharmacol* 2002; **12**:461–475.
- Klimek V, Stockmeier C, Overholser J, Meltzer HY, Kalka S, Dille G, et al. Reduced levels of norepinephrine transporters in the locus coeruleus in major depression. *J Neurosci* 1997; **17**:8451–8458.
- Tejani-Butt SM, Yang J, Zaffar H. Norepinephrine transporter sites are decreased in the locus coeruleus in Alzheimer's disease. *Brain Res* 1993; **631**:147–150.
- Schou M, Halldin C, Sovago J, Pike VW, Gulyas B, Mozley PD, et al. Specific *in vivo* binding to the norepinephrine transporter demonstrated with the PET radioligand, (*S,S*)-[¹¹C]MeNER. *Nucl Med Biol* 2003; **30**:QJ:707–714.
- Wilson AA, Johnson DP, Mozley PD, Hussey D, Ginovart N, Nobrega J, et al. Synthesis and *in vivo* evaluation of novel radiotracers for the *in vivo* imaging of the norepinephrine transporter. *Nucl Med Biol* 2003; **30**:85–92.
- Ding YS, Lin KS, Garza V, Carter P, Alexoff D, Logan J, et al. Evaluation of a new norepinephrine transporter PET ligand in baboons, both in brain and peripheral organs. *Synapse* 2003; **50**:345–352.
- Schou M, Halldin C, Sovago J, Pike VW, Hall H, Gulyas B, et al. PET evaluation of novel radiofluorinated reboxetine analogs as norepinephrine transporter probes in the monkey brain. *Synapse* 2004; **53**:57–67.
- Fowler J, Wang G, Logan J, Xie S, Volkow N, MacGregor R, et al. Selective reduction of radiotracer trapping by deuterium substitution: comparison of carbon-11-L-deprenyl and carbon-11-deprenyl-D2 for MAO B mapping. *J Nucl Med* 1995; **36**:1255–1262.
- Solin O, Eskola O, Hamill TG, Bergman J, Lehtikoinen P, Gronroos T, et al. Synthesis and characterization of a potent, selective, radiolabeled substance-P antagonist for NK1 receptor quantitation: ([¹⁸F]SPA-RQ). *Mol Imaging Biol* 2004; **6**:373–384.
- Carrio I. Cardiac neurotransmission imaging. *J Nucl Med* 2001; **42**:1062–1076.
- Farde L, Halldin C, Nagren K, Suhara T, Karlsson P, Schoeps KO, et al. Positron emission tomography shows high specific uptake of racemic carbon-11 labelled norepinephrine in the primate heart. *Eur J Nucl Med* 1994; **21**:345–347.
- Langer O, Valette H, Dolle F, Halldin C, Loc'h C, Fuseau C, et al. High specific radioactivity (1*R*,2*S*)-4-[¹⁸F]fluorometaraminol: a PET radiotracer for mapping sympathetic nerves of the heart. *Nucl Med Biol* 2000; **27**:233–238.
- Tipre DN, Lu JQ, Fujita M, Ichise M, Vines D, Innis RB. Radiation dosimetry estimates for the PET serotonin transporter probe ¹¹C-DASB determined from whole-body imaging in non-human primates. *Nucl Med Commun* 2004; **25**:81–86.
- Loevinger R, Watson E. *MIRD Primer for Absorbed Dose Calculations*. The Society of Nuclear Medicine; 1991.
- Cloutier RJ, Smith SA, Watson EE, Snyder WS, Warner GG. Dose to the fetus from radionuclides in the bladder. *Health Phys* 1973; **25**:147–161.
- Tipre D, Fujita M, Chin F, Seneca N, Vines D, Liow J, et al. Whole body biodistribution and radiation dosimetry estimates for the PET dopamine transporter probe ¹⁸F-FECNT in non human primates. *Nucl Med Commun* 2004; **25**:737–742.
- Meija A, Nakamura T, Itoh M, Hatazawa J, Ishiwata K, Ido T, et al. Absorbed dose estimates in positron emission tomography studies based on the administration of ¹⁸F labeled radiopharmaceuticals. *J Radiat Res* 1991; **32**:243–261.
- International Commission on Radiological Protection. *Radiological Protection and Safety in Medicine*. ICRP Publication 73. Ann ICRP 26. Oxford: Pergamon Press; 1996.
- Guidance on Medical Exposures in Medical and Biomedical Research. Radiation Protection 99. European Commission; 1998.